Pyrrole Hydrogenation over Rh(111) and Pt(111) Single-Crystal Surfaces and Hydrogenation Promotion Mediated by 1-Methylpyrrole: A Kinetic and Sum-Frequency Generation Vibrational Spectroscopy Study

*Christopher J. Kliewer, Marco Bieri and Gabor A. Somorjai**

Department of Chemistry, University of California, Berkeley, California 94720, and Materials Sciences Division, Lawrence Berkeley National Laboratory, Berkeley, California 94720

E-mail: somorjai@socrates.berkeley.edu

TITLE RUNNING HEAD: Pyrrole hydrogenation over Rh(111) and Pt(111)

RECEIVED DATE (to be automatically inserted after your manuscript is accepted if required according to the journal that you are submitting your paper to)

CORRESPONDING AUTHOR FOOTNOTE: Gabor A. Somorjai, Tel: 510-642-4053. Fax: 510-643-9668. E-mail: somorjai@socrates.berkeley.edu.

ABSTRACT. Sum frequency generation surface vibrational spectroscopy and kinetic measurements using gas chromatography have been used to study the adsorption and hydrogenation of pyrrole over both Pt(111) and Rh(111) single-crystal surfaces at Torr pressures (3 Torr pyrrole, 30 Torr H_2) to form pyrrolidine and the minor product butylamine. Over Pt(111) at 298K it was found that pyrrole adsorbs in an upright geometry cleaving the N-H bond to bind through the nitrogen evidenced by SFG data.

Over Rh(111) at 298K pyrrole adsorbs in a tilted geometry relative to the surface through the π-aromatic system. A pyrroline surface reaction intermediate, which was not detected in the gas phase, was seen by SFG during the hydrogenation over both surfaces. Significant enhancement of the reaction rate was achieved over both metal surfaces by adsorbing 1-methylpyrrole prior to reaction. SFG vibrational spectroscopic results indicate that reaction promotion is achieved by weakening the bonding between the N-containing products and the metal surface due to lateral interactions on the surface between 1-methylpyrrole and the reaction species, reducing the desorption energy of the products. It was found the ring-opening product butylamine was a reaction poison over both surfaces, but this effect can be minimized by treating the catalyst surfaces with 1-methylpyrrole prior to reaction. The reaction rate was not enhanced with elevated temperatures, and SFG suggests desorption of pyrrole at elevated temperatures.

1. Introduction

Catalytic reactions involving aromatic cyclic and heterocyclic molecules are important for the chemical industry for both fuel reforming and environmental concerns.[1] Due to the importance of surface interactions for heterogeneous catalysis, the adsorption of six-membered molecules, e.g. benzene and pyridine, has been studied on various metal surfaces.[2-6] Although five-membered ring systems are reaction intermediates in a number of catalytically important processes, they have received comparatively much less attention in surface science related research. This is partly explainable by the reduced stability of five-membered ring systems as compared to their six-membered analogues which makes the former less attractive for model studies since surface chemistry is expected to become more complex upon or following adsorption.

Pyrrole (C_4H_5N) is a five-membered aromatic ring system (Scheme 1) in which the lone pair of electrons of nitrogen is delocalized over the π-system of the ring. The adsorption of pyrrole on both Pt(111)[7] and Rh(111)[8] metal surfaces has been studied to provide some insight into the five-membered

heterocyclic bonding characteristics. The studies mentioned above showed that the adsorption geometry of pyrrole is sensitive to the type of metal substrate. Based on a NEXAFS study it was concluded that pyrrole adsorbs normal to the Pt(111) surface with the nitrogen as the anchoring point, which results in cleavage of the N-H bond.[7] Annealing of the pyrrole ad-layer in the absence of hydrogen further resulted in the dissociation of pyrrole leaving N-containing species on the Pt(111) surface. In contrast, on Rh(111), a study using angle resolved UV photoelectron spectroscopy (ARUPS), indicates that pyrrole is adsorbed at low temperature with its ring parallel to the surface, but a fraction of molecules splits off the N-hydrogen bond between 150 and 300 K allowing bonding interaction with the surface via the nitrogen.[8]

It has long been known that nitrogen containing compounds have inhibiting effects on the catalysts used for hydrogenation, due to their unshared pair of electrons. These poisoning effects can be reduced over Pt catalysts by conversion of these reactants into a form in which the nitrogen atom is shielded, e.g. by adding protic acids.[9-13] The hydrogenation of pyrrole derivatives was kinetically studied by Adkins and co-workers[14-16] over Raney nickel and other catalysts and later studies report on hydrogenation over supported precious metal catalysts (Pd/C, Ru/C, Rh/C, and Rh/Al_2O_3) in liquid phase by Hegedűs et al.[17-22] Under relatively mild reaction conditions (25-80 °C) and by using non-acidic solvents the hydrogenation of pyrrole derivatives showed higher activities on Rh than on Pt supported catalysts.

In this study, SFG vibrational spectroscopy and initial reaction turnover rates monitored by gas chromatography (GC) were used for the first time to investigate and verify surface species present during pyrrole hydrogenation (3 Torr of pyrrole) in the presence of excess hydrogen (30 Torr) over Rh(111) and Pt(111) single-crystal surfaces. Linear spectroscopies, such as infrared absorption, Raman, as well as electron spectroscopies typically cannot be employed under relevant catalytic reaction conditions (high pressure) due to the absorption by bulk gases, which masks the relatively small amount of absorption generated by adsorbed species at the catalyst surface. Because SFG is a second order nonlinear optical process, media with centrosymmetry and isotropic gases do not appear in the SFG spectrum under the electric dipole approximation.[23] Since bulk Rh and Pt have a center of inversion, its

contribution to the SFG signal is negligible. Because the symmetry is broken at the Rh and Pt single-crystal surfaces, SFG signal arises solely from the adsorbates. For these reasons, SFG is an ideal tool to monitor surface species under reaction conditions.

It has previously been reported in the literature that the co-adsorption of a large organic molecule on a catalyst surface can lead to enhanced hydrogenation reaction rates.[24-26] If the additive has a basic component that can interact laterally with neighboring adsorbates, it has been suggested this lateral adsorbate interaction can play a role in this promotion.[24] It has also been suggested that the co-adsorbed molecules can act as a hydrogen transfer agent to neighboring molecules, or to the catalyst surface increasing the surface coverage of hydrogen.[25,26] In this study, we found that adsorbing 1-methylpyrrole on the Rh(111) and Pt(111) surfaces prior to pyrrole hydrogenation significantly promotes the reaction rate. Gas chromatography measurements indicate that the production of ring-cracking products that poison the catalyst surface is significantly reduced in the presence of 1-methylpyrrole. Furthermore, blue-shifts of the amine vibrational modes to higher energies indicate that the interaction between nitrogen containing moieties of the reaction species and the surface is weakened when treated with 1-methylpyrrole prior to reaction favoring the desorption of reaction products and thus enhancing the hydrogenation rates.

2. Experimental Section

Materials

Prior to use, pyrrole (98%, Sigma-Aldrich Inc.), pyrrolidine (99%, Sigma-Aldrich Inc.), 1-methylpyrrole (99+%, SAFC Supply Solutions) and butylamine (≥99.5%, Fluka) were subjected to several freeze-pump-thaw cycles and the purities were checked by means of gas chromatography.

The high-pressure/ultra-high vacuum system

All experiments reported here were carried out in a high-pressure/ultrahigh-vacuum (HP/UHV) system. The UHV chamber is operated at a base pressure of 2×10^{-10} Torr and is isolated from the HP cell by a gate valve. The UHV system is equipped with an Auger electron spectrometer (AES), a quadrupole mass spectrometer (Stanford Research Systems) and an ion bombardment gun (Eurovac).

The HP cell consists of two CaF_2 conflat windows that allow transmission of infrared (IR), visible (VIS) and sum frequency radiation for sum frequency generation (SFG) experiments. The product gases in the HP cell are constantly mixed via a recirculation pump and kinetic data is acquired by periodically sampling the reaction mixture and analyzing the relative gas phase composition in a flame ionization detector (FID) of a gas chromatograph (Hewlett Packard HP 5890 on a 5% Carbowax 20M packed column). For the study of promotion effects mediated by 1-methylpyrrole, 100 millitorr 1-methylpyrrole was dosed into the HP cell and recirculated in the presence of the corresponding single-crystal for 5 min. The HP cell was then evacuated and the reactants were added to the HP cell.

Sample preparation

Prior to each experiment, the Rh(111) and Pt(111) crystal surfaces were cleaned in the UHV chamber by Ar^+ (700 eV for Rh and 1 keV for Pt) sputtering for 20 min at about 3 x 10^{-5} Torr of Ar. After sputtering, the crystals were heated to 1103 K in the presence of O_2 of 5 x 10^{-7} Torr and annealed at the same temperature for 2 min. The cleanliness of the crystal surfaces was verified by AES and the crystallographic structure verified with low energy electron diffraction (LEED). The samples were then transferred into the HP cell for SFG and kinetic studies.

Sum Frequency generation vibrational spectroscopy

For SFG measurements, an active/passive mode-locked Nd:YAG laser (Leopard D-20, Continuum) with a pulse width of 20 ps and a repetition rate of 20 Hz was used. The fundamental output at 1064 nm was sent through an optical parametric generation/amplification (OPA/OPG) stage where a tunable IR (2300—4000 cm^{-1}) and a second harmonic VIS (532 nm) beam were created. The IR (150 μJ) and VIS (200 μJ) beams were spatially and temporally overlapped on the crystal surface at angles of incidence of 55 and 60°, respectively, with respect to the surface normal. The generated SFG beam was collected and sent through a motorized monochromator equipped with a photomultiplier tube to detect the SFG signal intensity. The signal-to-noise ratio was further increased by using a gated integrator while the IR beam was scanned through the spectral region of interest. The SFG process is enhanced when the IR beam comes into resonance with a vibrational mode of a molecule adsorbed at the surface, giving rise to a

vibrational spectrum of adsorbed species. More information on the HP/UHV system and SFG measurement can be found elsewhere.[23,27-31]

3. Results and Discussion

3.1. Pyrrole Hydrogenation on Pt(111) and Rh(111) Single-Crystals under 3 Torr Pyrrole and 30 Torr Hydrogen: Turnover Rates, Selectivities, Deactivation, and Reaction Promotion by 1-Methylpyrrole.

Figure 1 displays the production of pyrrolidine as turnover rates (TOR, pyrrolidine molecules formed per metal surface atom per second) for both the Pt(111) (—■—) and Rh(111) (—●—) surfaces as a function of time under 3 Torr pyrrole and 30 Torr hydrogen at room temperature. Over both surfaces the major product was the full hydrogenation of the aromatic pyrrole ring to form pyrrolidine (see Scheme 1). Over Pt(111) the TOR at one hour reaction time at room temperature was found to be 0.049 (±0.003) and very little deactivation of the catalyst was observed, while over Rh(111) at room temperature and at one hour the TOR was 0.053 (±0.018) and the TOR deactivated by 54% during the first hour of reaction. The turnover rates over Pt(111) and Rh(111) in the gas phase were therefore very similar, with the only difference being that Rh(111) exhibits deactivation, while Pt(111) does not. Whereas, in the liquid phase work by Hegedűs et al,[17] Rh on carbon exhibited an initial rate 62.5 times faster than Pt on carbon for the hydrogenation of pyrrole derivatives. We further investigated the temperature dependence of this reaction ranging from 298-413 K over both surfaces, but the rate of formation of pyrrolidine was not enhanced with temperature, and at elevated temperatures reaction deactivation was observed.

Figure 1 demonstrates the significant effect adsorbing 1-methylpyrrole on the surface prior to reaction has on the rate of pyrrole hydrogenation over both surfaces. On the Rh(111) surface a 17 fold rate enhancement is achieved by exposing the crystal to 100 millitorr 1-methylpyrrole preceding the reaction (—▲—), and no deactivation was seen after six hours of reaction time. This is an indication that the 1-methylpyrrole does not leave the Rh(111) surface during the course of the reaction as the promotion does not deactivate. The Pt(111) (—♦—) surface also demonstrated a significantly enhanced initial rate,

by a factor of 17 fold, when 1-methylpyrrole is first adsorbed on the surface, but the reaction rate slows down by more than 80% within the first hour of hydrogenation.

Table 1 shows the selectivities for this reaction over both catalyst surfaces at 298K observed with GC. As can be seen, by breaking a N-C bond, the pyrrolidine ring can crack on the surface to form the minor product butylamine. Further cracking to lighter compounds is seen only on Rh(111), while Pt(111) exhibits the highest tendency for ring opening. The adsorption of 1-methylpyrrole on the metal surfaces prior to reaction affects the reaction selectivities. Over both surfaces the selectivity for the formation of butylamine is greatly reduced. Once again the effect of elevated temperatures was studied for the 1-methylpyrrole promoted pyrrole hydrogenations, but it led to a significant deactivation of the reaction, not following Arrhenius type behavior.

3.2. Surface Species during Reaction on Unpromoted Pt(111) and Rh(111): Sum Frequency Generation Vibrational Spectroscopy Results. The gas phase infrared spectrum for pyrrole exhibits only two vibrational resonances in the 2700-3600 cm^{-1} region, an aromatic N-H stretch at 3530 cm^{-1} and an aromatic C-H stretch at 3128 cm^{-1}.[32-34] Table 2 displays vibrational resonances for pyrrole,[32-35] pyrrolidine,[36] and butylamine[37,38] in the gas phase. The appearance of vibrational modes in the C-H region below 3000 cm^{-1} indicates hydrogenated products exist on the surface, as pyrrole has no such vibrational modes. Figure 2 shows the SFG vibrational spectra of 3 Torr pyrrole and 30 Torr hydrogen over Pt(111) at both 298 and 363K. The spectrum recorded at room temperature is characterized by nine vibrational resonances. The aromatic stretch at 3105 cm^{-1} indicates that an intact aromatic ring is adsorbed on the surface. The metal surface selection rule (MSSR)[39,40] states that vibrational modes parallel to a metal surface do not appear in the SFG vibrational spectrum, whereas vibrational modes with a component perpendicular to the surface are enhanced by the metal surface. Due to the appearance of the aromatic stretch in the spectrum we conclude that the aromatic ring must be standing with some component normal to the surface. Interestingly, there is no aromatic N-H stretch seen in this spectrum, but a strong C-H aromatic vibrational band. From this we can conclude that the pyrrole molecule adsorbs to the Pt(111) surface by cleaving the N-H bond, standing perpendicular to the

surface, maintaining the aromaticity of the ring as can be seen in Figure 3. This adsorption mode is an agreement with a previous NEXAFS work done by Tourillon et al.[7] The symmetric and asymmetric stretch of both the CH_3 and CH_2 groups can be seen for pyrrole hydrogenation on Pt(111). Firstly, this indicates that the hydrogenated products exist on the surface. Secondly, this is proof of the existence of the ring-opening product butylamine on the surface due to the clear presence of the CH_3 modes, which do not exist in the ring structure of pyrrolidine. A stretch also appears at 3055 cm^{-1} which is assigned to the vinylic stretch of pyrroline (Figure 3), which arises on the surface due to the hydrogenation of one of the double bonds in the pyrrole ring. Pyrroline is thus a surface reaction intermediate seen only in the SFG vibrational spectrum, as this product was not evolved in detectable amounts by GC during reaction. The N-H peaks seen from 3200 cm^{-1} to 3400 cm^{-1} on Pt(111) are all quite broad and do overlap with each other. However, three peaks are distinguishable at 3200 cm^{-1}, 3258 cm^{-1}, and 3380 cm^{-1}. The presence of these three peaks suggests a primary amine and agrees well with the vibrational spectrum of butylamine, and we assign these peaks to $2\delta(NH_2)$ = 3200 cm^{-1}, $\nu_{sym}(NH_2)$ = 3258 cm^{-1}, and $\nu_{asym}(NH_2)$ = 3380 cm^{-1}. The broadness of the features in this region suggests that there may be more N-H species present on the surface, such as the N-H stretch of pyrrolidine, but this cannot be elucidated from these studies. Spectra of pyrrole in the absence of excess hydrogen were also taken, but were identical to those recorded in the presence of excess hydrogen.

To investigate why this reaction shows deactivation upon heating rather than Arrhenius rate enhancement, the SFG vibrational spectrum was taken on Pt(111) at 363K (see Figure 2, top spectrum). Upon heating the Pt(111) to 363K, all peaks except those corresponding to CH_3 and CH_2 groups vanish. An explanation for this is that the pyrrole ring itself is not strongly bound and desorbs from the surface, and the other reactive intermediates on the surface (pyrroline, pyrrolidine, and butylamine) must either then be desorbed or become bound in such a way that nitrogen contains no hydrogen bonds, such as forming a relatively strong N=Pt bond. In either case, desorption or the formation of an N=Pt bond, this helps to explain the non-Arrhenius behavior of this reaction.

Figure 4 displays the SFG vibrational spectrum (bottom) of 3 Torr pyrrole and 30 Torr hydrogen on Rh(111). The CH_2 stretches are clearly seen at $\nu_{sym}(CH_2)$ = 2850 cm^{-1} and $\nu_{asym}(CH_2)$ = 2905 cm^{-1}. Similarly to Pt(111), a ν(=CH) peak can be seen at 3048 cm^{-1}, indicating the presence of the partially hydrogenated ring. The aromatic C-H stretch is seen at 3095 cm^{-1} indicating an intact aromatic ring adsorbed to the surface with a component perpendicular to it. This mode is 10 cm^{-1} further red-shifted than the aromatic C-H seen on Pt(111), which suggests a more electron donating interaction between the π-aromatic system and the Rh(111) surface than on the Pt(111) surface. The N-H modes on Rh(111) are very pronounced (see Figure 4), however the region from 3180 cm^{-1} to 3300 cm^{-1} becomes one broad feature comprised of several strong N-H vibrational modes. However, two bands are clearly visible at 3385 cm^{-1} and 3495 cm^{-1}. These are assigned to $\nu_{asym}(NH_2)$ = 3385 cm^{-1} and an aromatic N-H at 3495 cm^{-1}. Due to the fact that both the aromatic C-H and the aromatic N-H modes are seen on Rh(111) the proposed adsorption mode is tilted with respect to the surface bonding through the π-aromatic system (Figure 5). This suggested adsorption mode is also in agreement with work by Netzer et al.[8] which suggested the coexistence of both parallel and tilted pyrrole molecules on Rh(111) at room temperature. Though we can say with certainty that the tilted mode exists, we cannot rule out the possibility of a coexistence of a parallel adsorption mode based on the SFG vibrational results as such a molecule would not yield any SFG vibrational signature over a metal surface.

3.3. Surface Species During the Pyrrole Hydrogenation Reaction on Pt(111) and Rh(111) Promoted by the Adsorption of 1-Methylpyrrole Prior to Reaction: Sum Frequency Generation Vibrational Spectroscopy Results. The adsorption of 1-methylpyrrole over Pt(111) has been studied by Tourillon et al.[7] with NEXAFS, and it was found that 1-methylpyrrole is stable against dissociation on the surface, and was likely to desorb intact at elevated temperatures, while pyrrole was found to dissociate into N-containing species as the temperature was increased. The SFG vibrational spectrum of 5 Torr 1-methylpyrrole on Pt(111) was taken and can be seen in Figure 6. No N-H modes are seen in the spectrum, indicating that the molecule is much more stable on the Pt(111) surface than pyrrole

towards ring opening. The aromatic C-H stretch is seen at 3130 cm^{-1}, and the corresponding CH_3 and CH_2 stretches are also seen.

Figure 7 displays the spectrum of pyrrole hydrogenation on Pt(111) following an exposure to 100 millitorr of 1-methylpyrrole. To investigate the significant deactivation seen kinetically over Pt(111) pre-treated with 1-methylpyrrole the bottom spectrum was taken during the first hour of reaction, and the top spectrum was averaged from one to three hours after initiating the reaction. In the top spectrum, all of the major peaks seen for Pt(111) are once again present. However, the peaks corresponding to N-H modes are seen at $2\delta(NH_2)$ = 3220 cm^{-1}, $\nu_{sym}(NH_2)$ = 3300 cm^{-1}, and $\nu_{asym}(NH_2)$ = 3416 cm^{-1}. All of these vibrational modes are blue-shifted compared to unpromoted Pt(111) (see Table 3), indicating a weaker, less electron donating, interaction with the Pt(111) surface. This suggests that the co-adsorption with 1-methylpyrrole decreases the bonding interaction of the nitrogen containing portion of the product molecules with the surface, lowering the desorption energy, and reducing their residence time on the surface. In comparison with the bottom spectrum taken during the first hour of reaction, it is evident that that the intensities of the vibrational modes assigned to butylamine on the surface increase with time, as they are essentially absent in the bottom spectrum. Thus as the surface concentration of butylamine on Pt(111) increases, the rate of reaction for the formation of pyrrolidine decreases concomitantly. This suggests that butylamine is acting as a surface poison on Pt(111), being more strongly bound than reacting molecules, and using up the active sites.

The top spectrum in Figure 4 is that of 3 Torr pyrrole and 30 Torr hydrogen over Rh(111) which was recorded after exposing the surface to 100 millitorr 1-methylpyrrole prior to reaction. As can be seen, most of the stretches are identical to that of Rh(111) without the pre-treatment of 1-methylpyrrole except for those pertaining to the N-H stretches. The two distinguishable N-H bands are seen for $\nu_{asym}(NH_2)$ at 3410 cm^{-1} and for the aromatic N-H at 3510 cm^{-1}. This is a 25 cm^{-1} and 15 cm^{-1} blue shift in the wavenumber respectively (Table 3), when compared to pyrrole hydrogenation over Rh(111) without pre-adsorbed 1-methylpyrrole. This blue-shift is attributed to a weaker interaction between the Rh(111) surface and these N-H bonds.

The SFG vibrational spectroscopy results over both Rh(111) and Pt(111) suggest that the adsorption of 1-methylpyrrole on the surface prior to the pyrrole hydrogenation reaction promotes the reaction rate by weakening the interaction of the nitrogen containing portion of the product molecules with the surface, allowing them to desorb more readily. This would allow pyrrolidine to desorb before continuing on to form the ring-cracking product more frequently.

3.4. Reaction Deactivation by Butylamine. Clearly, a good catalyst should not be bound too strongly to reaction products, or competitive adsorption between reactants and products will reduce the reaction rate. In the case of pyrrole hydrogenation, the lone pair of electrons on the nitrogen atom is delocalized over the pyrrole molecule, but once one of the double bonds in the ring is hydrogenated, the nitrogen lone pair orbital is free to interact and bond with the metal surface. It was shown (Table 1) that the promotion of pyrrole hydrogenation by the adsorption of 1-methylpyrrole prior to reaction significantly reduced the ring-opening tendency to form butylamine. To test the poisoning properties of butylamine, a reaction mixture of 3 Torr pyrrole, 0.3 Torr butylamine, and 30 Torr hydrogen was reacted over a Rh(111) surface that had been dosed with 100 millitorr 1-methylpyrrole prior to reaction. This resulted in a TOR at one hour which was 62% slower than that of the reaction without the butylamine additive. To gain a more complete picture of the deactivation kinetics in this reaction the conversion of pyrrolidine to butylamine was also studied. 4 Torr pyrrolidine and 40 Torr hydrogen were reacted over Rh(111). In one hour, the Rh(111) converted 7.4% of the pyrrolidine to butylamine. When the same reaction was carried out over Rh(111) that was exposed to 100 millitorr 1-methylpyrrole prior to reaction, 0.7% of the pyrrolidine had been converted to butylamine after one hour. Thus, the adsorption of 1-methylpyrrole on the surface before the reaction resulted in a near 10 fold decrease in the ring-opening of pyrrolidine over Rh(111).

The SFG results during pyrrole hydrogenation indicated that over Pt(111) as the surface concentration of butylamine increased the reaction rate decreased. We can see here kinetically that the presence of butylamine in the reaction mixture over Rh(111) promoted with 1-methylpyrrole significantly decreases the reaction rate. Further, the co-adsorption of 1-methylpyrrole significantly inhibits the ring-opening of

pyrrolidine on the surface. This effect can also be seen when comparing the pyrrole hydrogenation reaction selectivities (Table 1), which show that the reaction promotion by 1-methylpyrrole is accompanied by a significant decrease in the selectivity for ring-opening to form butylamine. This may be attributed to a shorter residence time of the pyrrolidine product molecule on the surface, due to its weakened interaction with the surface, allowing it to desorb before cracking the ring more frequently.

4. Conclusions.

Using a combination of SFG vibrational spectroscopy and kinetic measurements, the adsorption geometry and hydrogenation pathway of pyrrole has been clarified over both Pt(111) and Rh(111) single-crystal surfaces during reaction at catalytically relevant pressures and temperatures. SFG results show that on Pt(111) the N-H bond of the pyrrole molecule is cleaved, and pyrrole binds through the nitrogen to the metal surface in an upright orientation. On Rh(111) a tilted adsorption geometry was found in which the pyrrole molecule binds to the metal surface through its aromatic π-electron system.

Further, it was found that pre-treating the metal surfaces with 1-methylpyrrole significantly promotes the pyrrole hydrogenation reaction over both metal surfaces. Rh(111) exhibited a 17 fold rate enhancement, and showed little reaction deactivation. Pt(111) exhibited rate enhancement but was quickly deactivated back to the rate seen without promotion. SFG vibrational spectroscopy results showed that as the pyrrole hydrogenation rate over Pt(111) pre-dosed with 1-methylpyrrole deactivated, its surface concentration of butylamine increased, acting as a surface poison. It was shown that the presence of co-adsorbed 1-methylpyrrole weakens the interaction of the N-H modes with the metal surfaces, indicating less electron donation from the nitrogen atom to the surface. This suggests that the rate enhancement observed by co-adsorbing 1-methylpyrrole during pyrrole hydrogenation is achieved by lowering the desorption energy of the N-containing products.

ACKNOWLEDGMENT

This work was supported by the Director, Office of Energy Research, Office of Basic Energy Sciences, and Materials Sciences Division of the U.S. Department of Energy under Contract DE-AC02-05CH11231. M. B. thanks the Swiss National Science Foundation (SNF) for financial support.

References

(1) Cooper, B. H.; Donnis, B. B. L. *Applied Catalysis a-General* **1996**, *137*, 203.

(2) Netzer, F. P.; Bertel, E.; Matthew, J. A. D. *Surface Science* **1980**, *92*, 43.

(3) Horsley, J. A.; Stohr, J.; Hitchcock, A. P.; Newbury, D. C.; Johnson, A. L.; Sette, F. *Journal of Chemical Physics* **1985**, *83*, 6099.

(4) Ogletree, D. F.; Vanhove, M. A.; Somorjai, G. A. *Surface Science* **1987**, *183*, 1.

(5) Weiss, P. S.; Eigler, D. M. *Physical Review Letters* **1993**, *71*, 3139.

(6) Bratlie, K. M.; Kliewer, C. J.; Somorjai, G. A. *Journal of Physical Chemistry B* **2006**, *110*, 17925.

(7) Tourillon, G.; Raaen, S.; Skotheim, T. A.; Sagurton, M.; Garrett, R.; Williams, G. P. *Surface Science* **1987**, *184*, L345.

(8) Netzer, F. P.; Bertel, E.; Goldmann, A. *Surface Science* **1988**, *199*, 87.

(9) Hamilton, T. S.; Adams, R. *Journal of the American Chemical Society* **1928**, *50*, 2260.

(10) Maxted, E. B.; Walker, A. G. *Journal of the Chemical Society* **1948**, 1093.

(11) Devereux, J. M.; Payne, K. R.; Peeling, E. R. A. *Journal of the Chemical Society* **1957**, 2845.

(12) Maxted, E. B.; Biggs, M. S. *Journal of the Chemical Society* **1957**, 3844.

(13) Freifelder, M. *Practical Catalytic Hydrogenation*; Wiley: New York, 1971.

(14) Signaigo, F. K.; Adkins, H. *Journal of the American Chemical Society* **1936**, *58*, 709.

(15) Rainey, J. L.; Adkins, H. *Journal of the American Chemical Society* **1939**, *61*, 1104.

(16) Adkins, H.; Wolff, I. A.; Palvic, A.; Hutchinson, E. *Journal of the American Chemical Society* **1944**, *66*, 1293.

(17) Hegedus, L.; Mathe, T.; Tungler, A. *Applied Catalysis a-General* **1996**, *147*, 407.

(18) Hegedus, L.; Mathe, T.; Tungler, A. *Applied Catalysis a-General* **1997**, *161*, 283.

(19) Hegedus, L.; Mathe, T.; Tungler, A. *Applied Catalysis a-General* **1997**, *153*, 133.

(20) Tungler, A.; Hegedus, L.; Hada, V.; Mathe, T.; Szepesy, L. *Chem. Ind.: Cat. Org. React.* **2001**, *82*, 425.

(21) Hegedus, L.; Mathe, T. *Applied Catalysis a-General* **2002**, *226*, 319.

(22) Hegedus, L.; Mathe, T.; Tungler, A. *Applied Catalysis a-General* **1996**, *143*, 309.

(23) Shen, Y. R. *The Principles of Nonlinear Optics*; John Wiley & Sons: New Jersey, 2003.

(24) Bond, G.; Meheux, P. A.; Ibbotson, A.; Wells, P. B. *Catalysis Today* **1991**, *10*, 371.

(25) Jackson, S. D.; Hardy, H.; Kelly, G. J.; Shaw, L. A. The effect of co-adsorbates on activity/selectivity in the hydrogenation of aromatic alkynes. In *Heterogeneous Catalysis and Fine Chemicals Iv*, 1997; Vol. 108; pp 305.

(26) Jackson, S. D.; Munro, S.; Colman, P.; Lennon, D. *Langmuir* **2000**, *16*, 6519.

(27) Bratlie, K. M.; Flores, L. D.; Somorjai, G. A. *Surface Science* **2005**, *599*, 93.

(28) Kung, K. Y.; Chen, P.; Wei, F.; Rupprechter, G.; Shen, Y. R.; Somorjai, G. A. *Review of Scientific Instruments* **2001**, *72*, 1806.

(29) Yang, M. C.; Tang, D. C.; Somorjai, G. A. *Review of Scientific Instruments* **2003**, *74*, 4554.

(30) Shen, Y. R. *Annual Review of Physical Chemistry* **1989**, *40*, 327.

(31) Shen, Y. R. *Nature* **1989**, *337*, 519.

(32) Klots, T. D.; Chirico, R. D.; Steele, W. V. *Spectrochimica Acta Part a-Molecular and Biomolecular Spectroscopy* **1994**, *50*, 765.

(33) Lord, R. C.; Miller, F. A. *Journal of Chemical Physics* **1942**, *10*, 328.

(34) Mellouki, A.; Lievin, J.; Herman, M. *Chemical Physics* **2001**, *271*, 239.

(35) Mellouki, A.; Georges, R.; Herman, M.; Snavely, D. L.; Leytner, S. *Chemical Physics* **1997**, *220*, 311.

(36) Evans, J. C.; Wahr, J. C. *Journal of Chemical Physics* **1959**, *31*, 655.

(37) Sokoll, R.; Hobert, H.; Schmuck, I. *Journal of the Chemical Society-Faraday Transactions I* **1986**, *82*, 3391.

(38) Teixeira-Dias, J. J. C.; de Carvalho, L. A. E. B.; da Costa, A. M. A.; Lampreia, I. M. S.; Barbosa, E. F. G. *Spectrochimica Acta Part A: Molecular Spectroscopy* **1986**, *42*, 589.

(39) Dignam, M. J.; Moskovit.M; Stobie, R. W. *Transactions of the Faraday Society* **1971**, *67*, 3306.

(40) Pearce, H. A.; Sheppard, N. *Surface Science* **1976**, *59*, 205.

Scheme 1

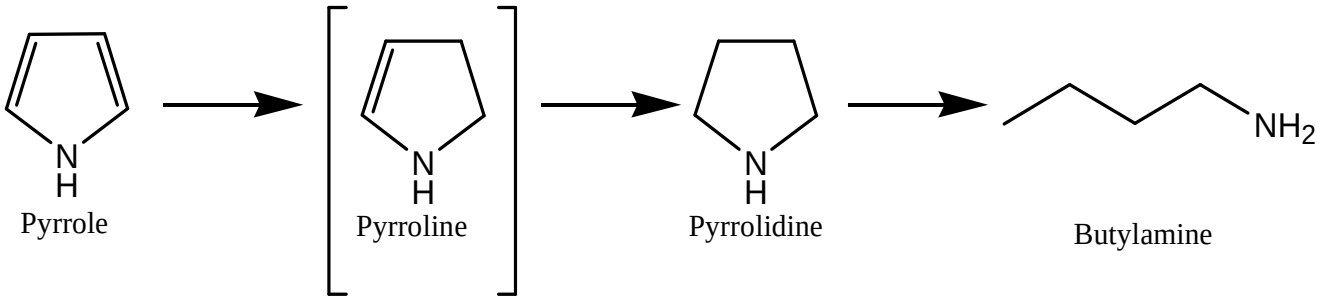

Pyrrole Pyrroline Pyrrolidine Butylamine

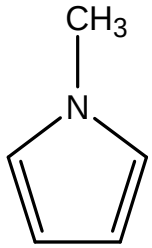

1-Methylpyrrole

Table 1. Selectivities of reaction products (given in %) after one hour of pyrrole hydrogenation (3 Torr pyrrole, 30 Torr H_2) over the corresponding catalyst surfaces.

Catalyst	pyrrolidine (%)	butylamine (%)	light cracking products (%)
Pt(111)	95.4	4.6	0
Rh(111)	97.7	1.5	0.8
Pt(111) pre-adsorbed with 1-methylpyrrole	99.3	0.7	0
Rh(111) pre-adsorbed with 1-methylpyrrole	99.9	0.1	0

Table 2. Summary of gas-phase vibrational modes (given in cm^{-1}) of pyrrole,[32,34,35] pyrrolidine,[36] and butylamine[37,38] in the spectral region between 2700 and 3600 cm^{-1}.

Assignment	pyrrole	pyrrolidine	Butylamine
$\nu_{sym}(CH_2)$		2825 and 2882	2858
$\nu_{sym}(CH_3)$			2868
$\nu_{asym}(CH_2)$		2967	2908
$\nu_{asym}(CH_3)$			2960
$\nu_{aromatic}(CH)$	3128		
$2\delta(NH_2)$			3180
$\nu_{sym}(NH_2)$			3340
ν (NH)		3367	
$\nu_{asym}(NH_2)$			3403
$\nu_{aromatic}(NH)$	3530		

Table 3. Summary and assignments of SFG vibrational modes observed during pyrrole hydrogenation (3 Torr pyrrole, 30 Torr H_2, see Figs. 2,4,6 and 7) over the corresponding catalyst surface. "MP" refers to the surface pre-adsorbed with 1-methylpyrrole. Vibrational frequencies are given in cm^{-1}.

Assignment	Pt(111)	Pt(111) with MP	Rh(111)	Rh(111) with MP
$\nu_{sym}(CH_2)$	2840		2850	2850
$\nu_{sym}(CH_3)$	2870	2860		
$\nu_{asym}(CH_2)$	2918	2918	2905	2905
$\nu_{asym}(CH_3)$	2962	2957		
ν(=CH)	3055		3048	3045
$\nu_{aromatic}$(CH)	3105	3110	3095	3095
$2\delta(NH_2)$	3200	3220	3180-3320	3180-3320
$\nu_{sym}(NH_2)$	3260	3300		
ν(NH)				
$\nu_{asym}(NH_2)$	3380	3416	3385	3410
$\nu_{aromatic}$(NH)			3495	3510

Figure Captions

Scheme 1

Reaction Mechanism (Top) and Structure of 1-Methylpyrrole (Bottom)

Figure 1

Turnover rates (pyrrolidine molecules formed per metal surface atom per second) for the formation of pyrrolidine as a function of time over Pt(111) (—■—) and Rh(111) (—●—) (included in both plots) as compared with Pt(111) dosed with 100 millitorr 1-methylpyrrole prior to reaction (—♦—) and Rh(111) dosed with 100 millitorr 1-methylpyrrole prior to reaction (—▲—) under 3 Torr pyrrole and 30 Torr H_2.

Figure 2

SFG vibrational spectra recorded during pyrrole hydrogenation (3 Torr pyrrole, 30 Torr H_2) over Pt(111). The spectrum depicted at the bottom was recorded at 298 K and the one depicted on top at 363 K.

Figure 3

Proposed molecular adsorption and reaction pathway over Pt(111). Pyrrole adsorbs perpendicularly by cleaving the N-H bond. Once the aromaticity is broken by the hydrogenation of one of the double bonds, the molecule binds to the Pt(111) surface through the lone pair of electrons on the nitrogen. The subsequent hydrogenation of the ring yields pyrrolidine molecules, some fraction of which may undergo ring-opening and hydrogenation to yield butylamine before desorption.

Figure 4

The bottom spectrum (—○—) is the SFG vibrational spectrum of 3 Torr pyrrole and 30 Torr hydrogen on Rh(111). The top spectrum (—△—) is of 3 Torr pyrrole and 30 Torr hydrogen on Rh(111) that was dosed with 100 millitorr 1-methylpyrrole prior to reaction.

Figure 5

Proposed molecular adsorption and reaction pathway over Rh(111). Pyrrole adsorbs in a tilted geometry to the surface bonding through the aromatic π system. Once the aromaticity is broken by hydrogenating one of the ring double bonds, the molecule binds to the Rh(111) surface through the lone pair of electrons on nitrogen, which is followed by ring saturation. The molecule may either then desorb to form pyrrolidine, or crack the ring to form butylamine and desorb. On Rh(111) a very small fraction of molecules further decomposes to lighter products.

Figure 6

SFG vibrational spectrum recorded under 5 Torr 1-methylpyrrole over Pt(111).

Figure 7

SFG vibrational spectra of 3 Torr pyrrole and 30 Torr hydrogen on Pt(111) after exposing the surface to 100 millitorr 1-methylpyrrole for five minutes. The bottom spectrum (—○—) was taken within one hour of reaction time. The top scpectrum (—△—) was taken from one to three hours.

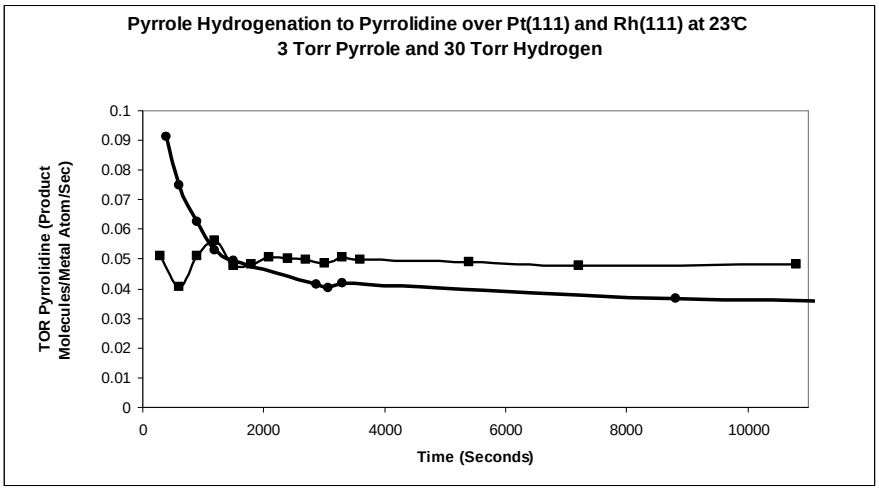
Pyrrole Hydrogenation to Pyrrolidine over Pt(111) and Rh(111) at 23℃
3 Torr Pyrrole and 30 Torr Hydrogen
TOR Pyrrolidine (Product Molecules/Metal Atom/Sec)
0.1
0.09
0.08
0.07
0.06
0.05
0.04
0.03
0.02
0.01
0
0
2000
4000
6000
8000
10000
Time (Seconds)

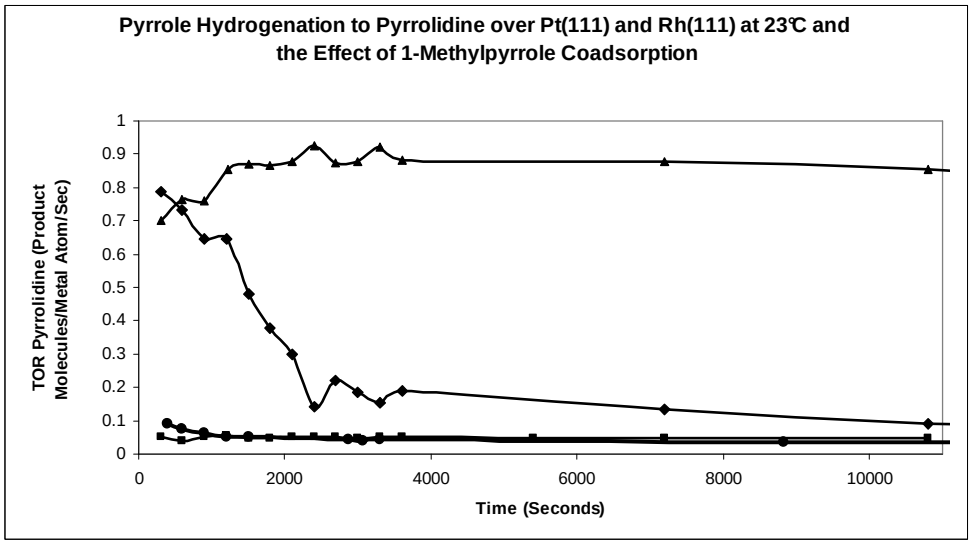
Pyrrole Hydrogenation to Pyrrolidine over Pt(111) and Rh(111) at 23℃ and
the Effect of 1-Methylpyrrole Coadsorption
TOR Pyrrolidine (Product Molecules/Metal Atom/Sec)
1
0.9
0.8
0.7
0.6
0.5
0.4
0.3
0.2
0.1
0
0
2000
4000
6000
8000
10000
Time (Seconds)

Figure 1

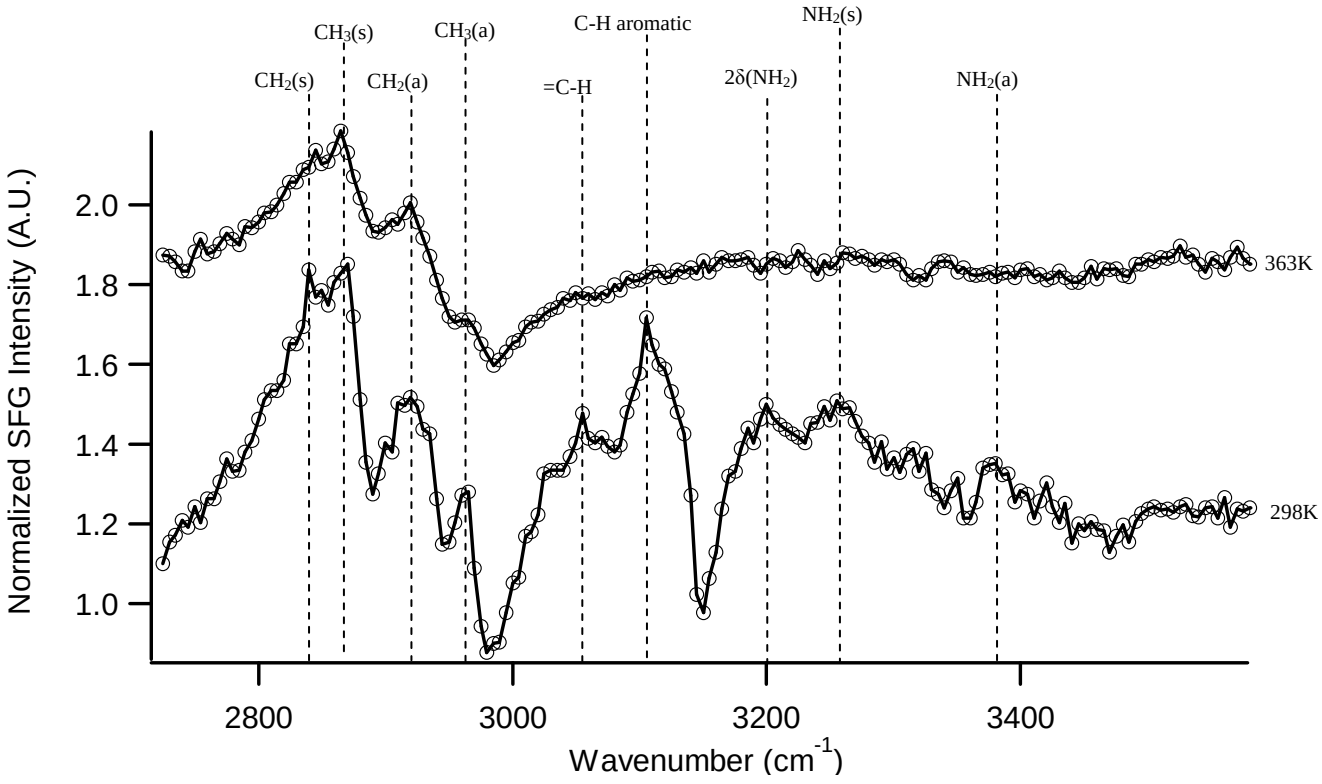
CH3(s)
CH3(a)
C-H aromatic
NH2(s)
CH2(s)
CH2(a)
=C-H
2δ(NH2)
NH2(a)
Normalized SFG Intensity (A.U.)
2.0
1.8
1.6
1.4
1.2
1.0
363K
298K
2800
3000
3200
3400
Wavenumber (cm-1)

Figure 2

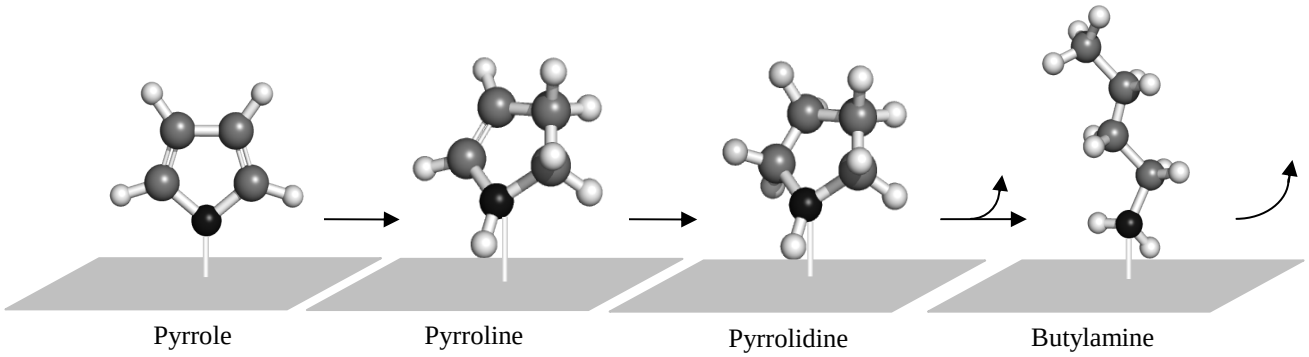

Figure 3

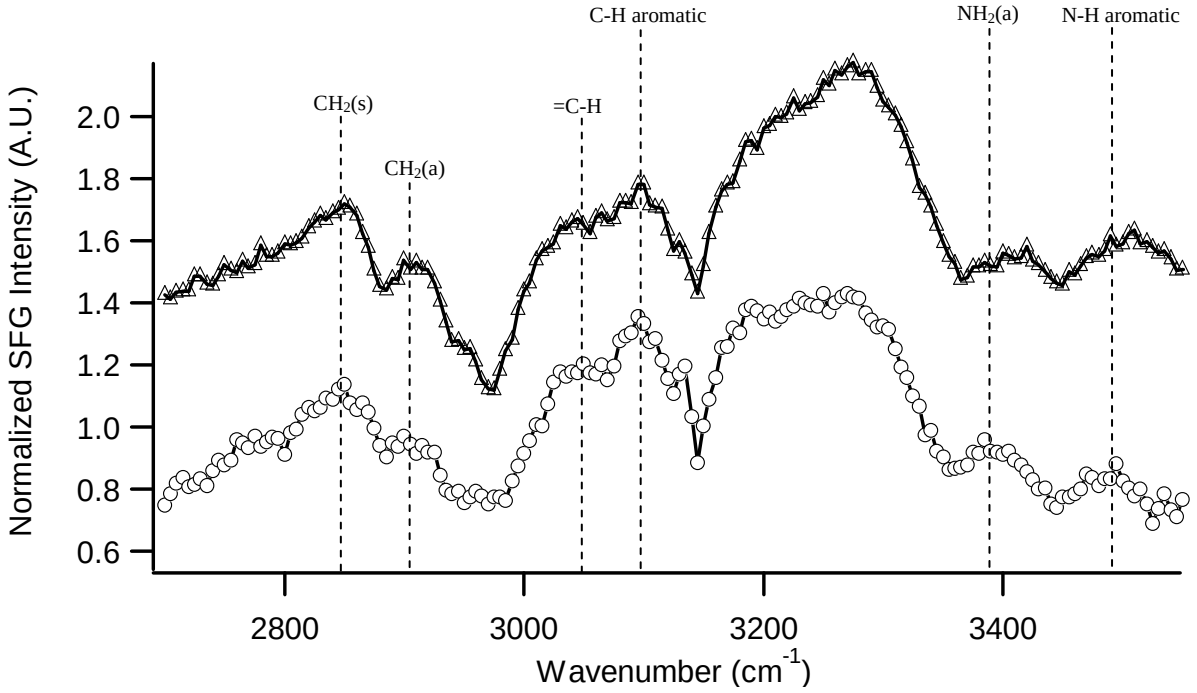
C-H aromatic
NH2(a)
N-H aromatic
CH2(s)
=C-H
CH2(a)
Normalized SFG Intensity (A.U.)
2.0
1.8
1.6
1.4
1.2
1.0
0.8
0.6
2800
3000
3200
3400
Wavenumber (cm-1)

Figure 4

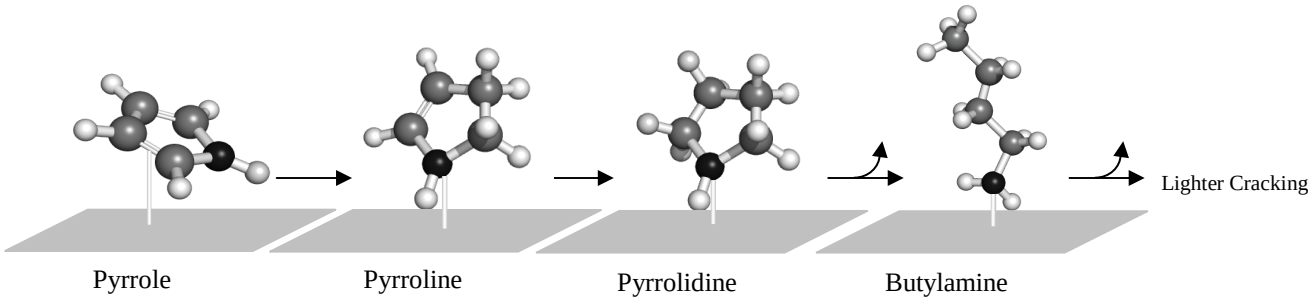
Lighter Cracking
Pyrrole
Pyrroline
Pyrrolidine
Butylamine

Figure 5

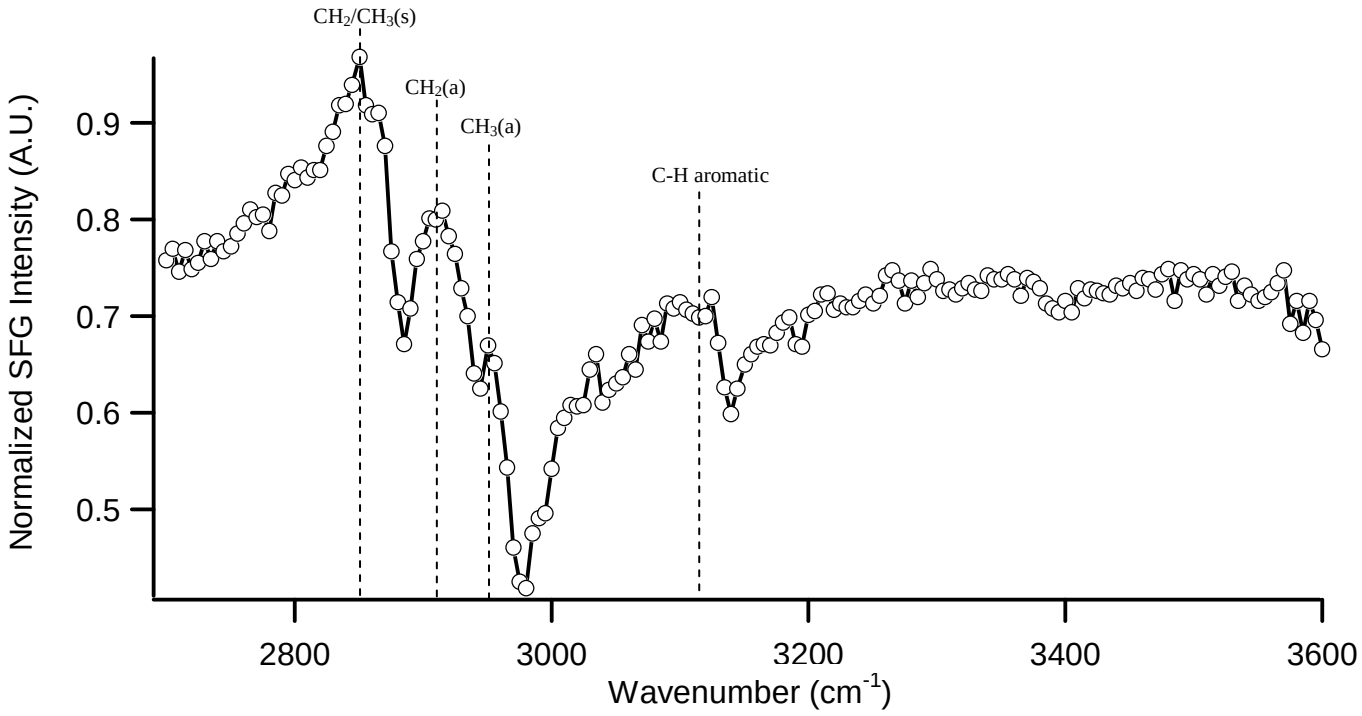
CH2/CH3(s)
CH2(a)
CH3(a)
C-H aromatic
Normalized SFG Intensity (A.U.)
0.9
0.8
0.7
0.6
0.5
2800
3000
3200
3400
3600
Wavenumber (cm-1)

Figure 6

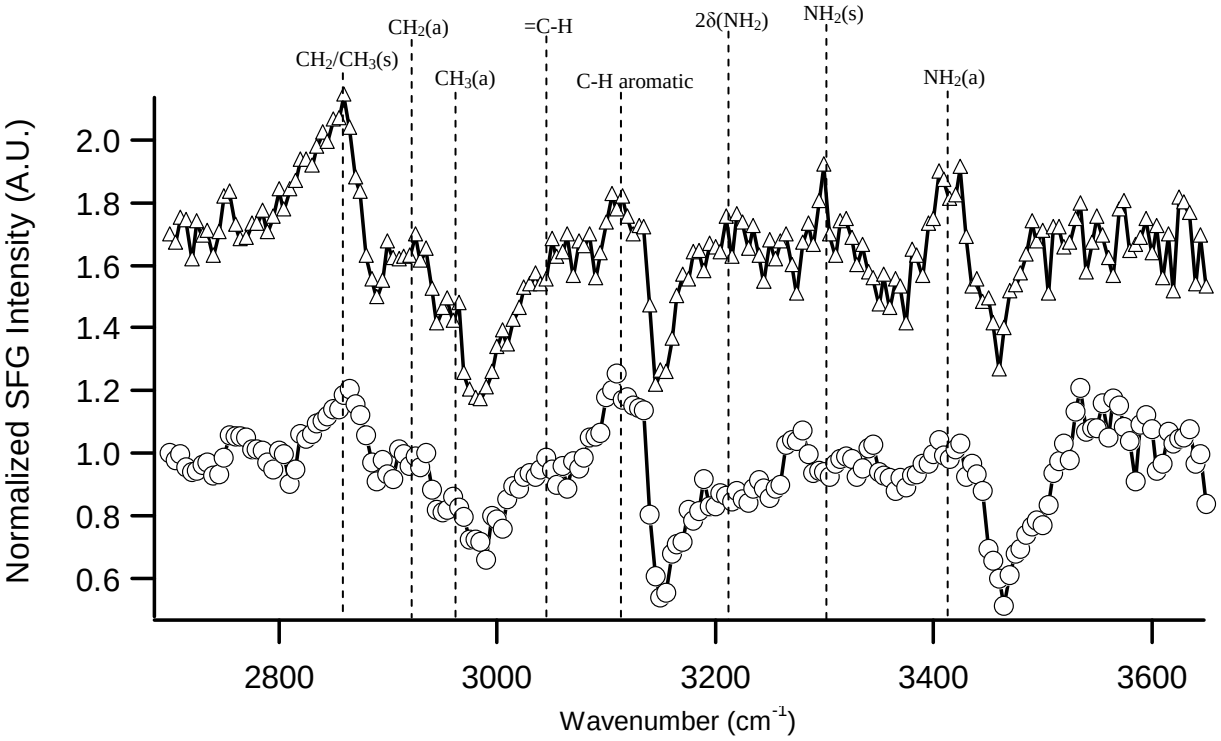
CH2/CH3(s)
CH2(a)
CH3(a)
=C-H
C-H aromatic
2δ(NH2)
NH2(s)
NH2(a)
Normalized SFG Intensity (A.U.)
2.0
1.8
1.6
1.4
1.2
1.0
0.8
0.6
2800
3000
3200
3400
3600
Wavenumber (cm-1)

Figure 7